Coherent Structure Formation in Turbulent Thermal Superfluids

Demosthenes Kivotides
Department of Mathematics, University of Newcastle, Newcastle upon Tyne, NE1 7RU, United Kingdom
(Received 22 February 2006; published 3 May 2006)

By means of numerical calculations, we show that in turbulent thermal superfluids the normal fluid induces coherent bundles of quantized line vortices in the superfluid. These filamentary structures are formed in between the normal fluid vortices, acquiring eventually comparable circulation. They are self-stretched and evolve according to self-regulating dynamics. Their spectrum mimics the normal fluid spectrum with the mutual friction force exciting the large scales and damping the small scales. Strongly interacting triads of them merge sporadically into stronger, braided vortex filaments, inducing strong fluctuations in the system's energetics. A theoretical account of the system's statistical mechanics is proposed.

DOI: 10.1103/PhysRevLett.96.175301 PACS numbers: 67.40.Vs, 47.37.+q

In turbulent thermal superfluids [1,2], recirculating superfluid motions induced by quantized vortices exchange (via mutual friction forces) energy and momentum with normal fluid eddies. At present, even the most elementary issues about the physics of such flows have not been resolved in a definite way. Among these issues one could mention scaling laws in the energy spectra of both fluids, the energetics of the mutual friction force, as well as the structure of superfluid vorticity. In this Letter, we calculate how normal turbulent eddies induce turbulence in the superfluid by causing a single initial superfluid vortex ring to grow and develop into a complex tangle. We show that this process, referred to as the thermal superfluid dynamo, is an appropriate context for a satisfactory resolution of the aforementioned issues. Mathematical models of thermal superfluids require separate dynamical equations for the superfluid and the normal fluid. Lately, a number of studies [3,4] have suggested that homogeneous isotropic turbulent normal flows are characterized by filamentary excitations of the incoherent vorticity background state fluctuations. Because of their near singular nature, these coherent vorticity structures carry most of the energy and enstrophy of the flow and are conjectured to correspond to the inertial range of turbulence and determine the Kolmogorov spectrum [5,6]. Based on these studies, a model was developed [6–10] that describes normal fluid turbulence in terms of coherent structures (vortices) and compares well with Navier-Stokes phenomenology since it reproduces, among other, the Kolmogorov scalings of the energy spectrum and the third order longitudinal structure function. By adopting this model in the present study, we describe both the normal fluid and the superfluid as vortex dynamical systems.

The latter are fully determined by the evolution of the three dimensional representation $\boldsymbol{X}_f(\xi_f, t)$ of a vortex tangle $\mathcal{L}_f$, where ξ_f is the arclength parametrization along the vortex loops, t is time, and the index f is $f = n$ for normal fluids and $f = s$ for superfluids. The evolution equation for $\boldsymbol{X}_s(\xi_s, t)$ is given by [11]

$$\frac{\partial \boldsymbol{X}_s}{\partial t} = h\boldsymbol{V}_s + h_\times \boldsymbol{X}_s' \times (\boldsymbol{V}_n - \boldsymbol{V}_s) - h_{\times\times} \boldsymbol{X}_s' \times (\boldsymbol{X}_s' \times \boldsymbol{V}_n), \tag{1}$$

where $\boldsymbol{V}_n$ is the normal fluid velocity and the superfluid velocity $\boldsymbol{V}_s$ is given by the Biot-Savart integral

$$\boldsymbol{V}_s(\boldsymbol{x}) = -\frac{\kappa}{4\pi}\int_{\mathcal{L}_s} d\xi_s \frac{\boldsymbol{X}_s' \times (\boldsymbol{X}_s - \boldsymbol{x})}{|\boldsymbol{X}_s - \boldsymbol{x}|^3}. \tag{2}$$

Here, $\boldsymbol{X}_s' \equiv \partial \boldsymbol{X}_s / \partial \xi_s$ is the unit tangent vector (indicating the direction of the singular superfluid vorticity), κ is the quantum of circulation, and h, $h_\times$, $h_{\times\times}$ are known dimensionless mutual friction parameters.

The model for the normal fluid vortices is described in detail in [6]:

$$\frac{\partial \boldsymbol{X}_n}{\partial t} = \boldsymbol{V}_n, \tag{3}$$

where $\boldsymbol{V}_n$ is the Biot-Savart velocity

$$\boldsymbol{V}_n(\boldsymbol{x}) = -\frac{1}{4\pi}\int_{\mathcal{L}_n} \frac{(\boldsymbol{x} - \boldsymbol{X}_n) \times \boldsymbol{\omega}_n(\boldsymbol{X}_n) d\boldsymbol{X}_n}{|\boldsymbol{x} - \boldsymbol{X}_n|^3}, \tag{4}$$

where $\boldsymbol{\omega}_n$ is the normal fluid vorticity vector. The employed $\boldsymbol{\omega}_n$ formula [6] takes into account the finite core of the filaments, as well as variations of the latter along the vortices (thus capturing the physics of vortex stretching). The viscous effects are handled by the core-spreading scheme [6]. When two normal fluid filaments approach closer than a fraction of their corresponding core radii, they reconnect according to the method of [12]. The calculations are done for helium II and $T = 1.3$ K thus $\kappa = 9.97 \times 10^{-4}$ cm^2/s, $h = 0.97824$, $h_\times = 0.04093$, $h_{\times\times} = 0.02175$ and the viscosity of the normal fluid is $\nu_n = 2.3303 \times 10^{-3}$ cm^2/s. The normal fluid Reynolds number $\mathrm{Re}_\gamma = \gamma/\nu_n$ (where $\gamma = 932.12 \times 10^{-4}$ cm^2/s is the circulation of the normal fluid vortices) is $\mathrm{Re}_\gamma = 40$. One notes that since $\gamma/\kappa = 93.492$, one normal fluid vortex is as strong as approximately 100 aligned superfluid vortices put together.

Because of algorithmic and computational complexity, we cannot compute here the fully consistent dynamics of the combined vortex systems. Instead, we solve a lesser problem that is defined as follows [6]: We choose a cubic computational domain of size $l_b = 0.1$ cm. Then, we place in it a number of normal vortex loops set at random locations and orientations with circulation γ defined above. The loops evolve according to Eq. (3) and undergo a large number of reconnections, quickly forming a time-dependent turbulent tangle. By checking the statistics of the vortex system, we determine when a statistically isotropic and homogeneous turbulence state with the appropriate Kolmogorov statistics is achieved [6]. Such a state is shown in Fig. 1 (top). For clarity, this figure shows only a fraction (0.13) of the actual tube radii. We then keep this normal turbulent flow constant in time while we investigate its effect, via mutual friction, on a single initial superfluid vortex ring. It will be shown that this lesser problem could be consistently considered to model the effects of the largest, more energetic, normal fluid eddies on the superfluid vortices.

FIG. 1 (color online). Static normal fluid vortex configuration (top) and typical superfluid vortex tangle (bottom, $t = 1.472$ s).

Both vortex systems satisfy periodic boundary conditions. The mesh size along the superfluid vortices is $\Delta\xi = l_b/48 = 0.1/48 = 2.08 \times 10^{-3}$ cm and its associate wave number is $k_{\Delta\xi} \approx 480$ cm^{-1}. As the vortices grow during their evolution, more discretization points are added along their contours, keeping the resolution constant and equal to $\Delta\xi$. Because of this, the number of mesh points grows from the initial value $N = 75$ to the final value $N \approx 90\,000$. The time step is chosen so that the fastest Kelvin waves allowed by the spatial discretization are well resolved. This requirement determines $\Delta t = 3.137 \times 10^{-4}$ s. In analogy with magnetohydrodynamics (MHD), one can call this problem the kinematic superfluid dynamo since it is expected that the initial seed superfluid vorticity and energy will be amplified by the normal fluid flow. Indeed, the initial superfluid ring is distorted and its length grows until close to $t = 1$ s, after 3200 time steps, the first obvious signs of superfluid line vortex conglomeration into bundles appear. Note that when this time is matched with an appropriate normal vortex motion time $\tau = (\gamma/R^2)^{-1}$, it gives a corresponding curvature radius $R = 0.3$ cm. This radius is comparable with the size of the computational box. Definitely, in a typical turbulent normal vortex system there would be vortices with larger curvature radii [8]. The less curved these vortices are, the more plausibly could be approximated as ‘‘static’’ during an interval of 1 s. Moreover, the velocity fields induced by them correspond to large scale eddy motions and therefore, since the spectrum scales like $k^{-5/3}$, to higher energies than the energies of the velocity fields induced by the highly curved and faster evolving vortices. Consequently, in agreement with the aforementioned interpretation of the present model, their more energetic velocity fields could be conjectured to organize the superfluid vortices along the lines depicted here. A typical superfluid tangle configuration is shown in Fig. 1 (bottom). At this time, $t = 1.472$ s, the superfluid vortex length L which initially was $L_0 = 0.15$ cm has grown up to $L_f = 153.951$ cm. The intervortex spacing is $\delta = 2.548 \times 10^{-3}$ cm and the corresponding wave number is $k_\delta \approx 392$. Evidently, linear coherent structures of quantized vortices thread the whole system. We have verified that the most prominent of these filaments are bundles of 35–40 lines of aligned vorticity, thus their circulation is comparable to that of the normal vortices.

Figure 2 (middle) shows the average values of the respective contributions of Biot-Savart law and mutual friction force to superfluid vortex dynamics, as well as the evolution of the superfluid kinetic energy E_s. It is observed that initially the mutual friction force outweighs, on average, the Biot-Savart law. However, at vortex bundle formation time, $t \approx 1$ s, the two effects are approximately balanced and, subsequently, the Biot-Savart contribution

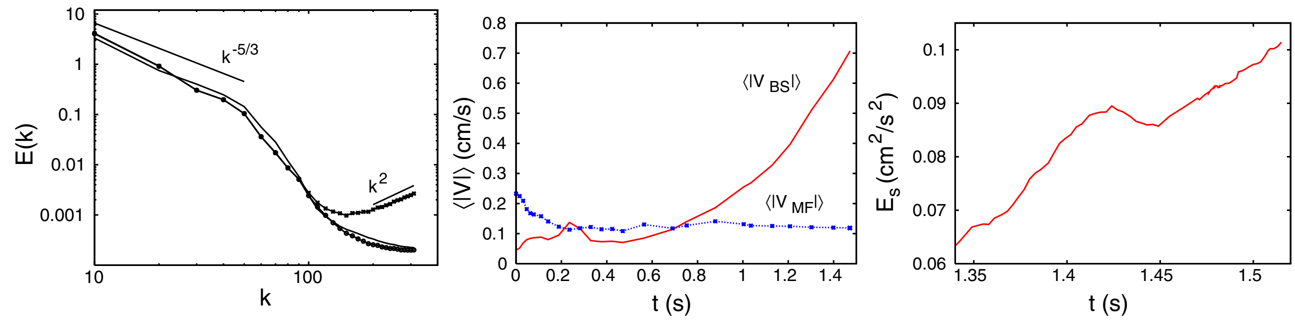

FIG. 2 (color online). Left: superfluid energy spectrum at $t = 1.4178$ s (circled line), $t = 1.4209$ s (starred line), and normal fluid energy spectrum (plain line); due to the difference in the two energies, the comparison of their scalings was made possible by multiplying the superfluid spectra by a factor 35. Middle: average magnitudes of contributions to the superfluid vortex dynamics ($\langle|\boldsymbol{V_{BS}}|\rangle = \langle|h\boldsymbol{V_s}|\rangle$, $\langle|\boldsymbol{V_{MF}}|\rangle = \langle|h_\times \boldsymbol{X}_s' \times (\boldsymbol{V_n} - \boldsymbol{V_s})|\rangle + \langle|h_{\times\times}\boldsymbol{X}_s' \times (\boldsymbol{X}_s' \times \boldsymbol{V_n})|\rangle$). Right: evolution of the superfluid kinetic energy E_s.

dominates. Therefore, structure formation is the outcome of dominant mutual friction action during the initial phases of the dynamo. This explains the absence of vortex structures in numerical calculations of pure superfluid vortex tangles ($T \rightarrow 0$ K). The dynamics of superfluid energy E_s are shown in Fig. 2 (right). A gradual reduction in the growth rate of superfluid energy is observed. A similar phenomenon occurs in the evolution of the superfluid vortex length. This can be understood by noticing that as the superfluid bundles grow stronger, they develop self-regulating dynamics which decorrelate vortex motion from mutual friction action. Although mutual friction remains the net contributor to the growth of superfluid energy, its efficiency ought to decline.

In order to elaborate a theory for the energetics of the system, we have calculated first the enstrophy production rate $\langle\phi\rangle = \langle\sum_{i=1}^{3} \Lambda_i \cos^2(\boldsymbol{X}_s', \boldsymbol{\Lambda_i})\rangle$ [8,13]. Since $\langle\phi\rangle = 68.129\ \mathrm{s}^{-1}$, it follows that the superfluid vortex bundles are, on average, self-stretched and they could develop an inertial range with a Kolmogorov scaling and accompanying energy cascade from large eddies to small. This is indeed the case, as indicated by the circled line spectrum of Fig. 2 (left) which refers to $t \approx 1.4178$ s and is representative of what is usually observed at other times. Since the observed cutoff in this spectrum is much smaller than $k_{\Delta\xi}$, the numerical resolution along the vortices is adequate for the present flow. Taking into account that the dynamics of the superfluid bundles are dominated by the inviscid Biot-Savart interactions, the observed spectrum seems at first paradoxical. This is because the Kolmogorov scaling of normal fluids is the effect of viscous stress induced small scale damping that keeps the system energetics constantly out of statistical equilibrium. In contrast, although (truncated) inviscid Euler dynamical systems do exhibit initially the formation of a Kolmogorov like inertial range, such systems are eventually thermalized. In particular, starting from the small scales, they develop the scaling $E_s(k) \propto k^2$ predicted by equilibrium statistical mechanics [14]. Why then is the superfluid spectrum similar to a normal fluid spectrum?

In order to answer this question we need to understand the energetics of the mutual friction force. The key observation is that around $t \approx 1.42$ s the superfluid energy decreases (Fig. 2, right). That is, for a particular interval of time, mutual friction work is a net energy sink for the superfluid system. Figure 2 (left) shows the superfluid energy spectrum (starred line, $t = 1.4209$ s), just before the observed superfluid energy reduction. The scaling $E_s(k) \propto k^2$ is observed at small scales. We have verified that as E_s decreases at subsequent times, the $E_s(k) \propto k^2$ scaling disappears and the spectrum returns to its typical, normal-fluid-like shape with the high k cutoff. This observation indicates that the mutual friction extracts energy from the smallest superfluid scales and transfers it to the normal fluid.

With this crucial information, we can explain the energetics of the flow: We need to discriminate between the inertial range, large scale energy $E_s^<$, and the small scale energy $E_s^>$. $E_s^<$ increases due to mutual friction input rate Q and decreases due to the superfluid vortex stretching induced energy flux F from small to large wave numbers. Since $E_s^<$ increases due to the dynamo effect, we must have that $|Q| - |F| > 0$. On the other hand, $E_s^>$ increases because of energy flux F cascading from the large scales and decreases because of mutual friction induced damping rate D. Since $E_s^>$ increases due to the dynamo effect, it must be $|F| - |D| > 0$, so typically $|Q| > |F| > |D|$. However, due to the statistical nature of the system's energetics, a fluctuation during which $|F| \gg |D|$ might temporarily be induced by rare strong bundle stretching events. The strong vortex interactions during the merging of three superfluid bundles into a vortex braid (Fig. 3, to be discussed later), is a particular example of such an event. Such a fluctuation takes place at times before $t = 1.4209$ s leading to energy accumulation at small scales and subsequent equipartition. These explain the observed partially thermalized superfluid spectrum at $t \approx 1.42$ s (Fig. 2, left). Subsequently, because of their increased energy, the smallest superfluid eddies start giving energy to the normal fluid via mutual

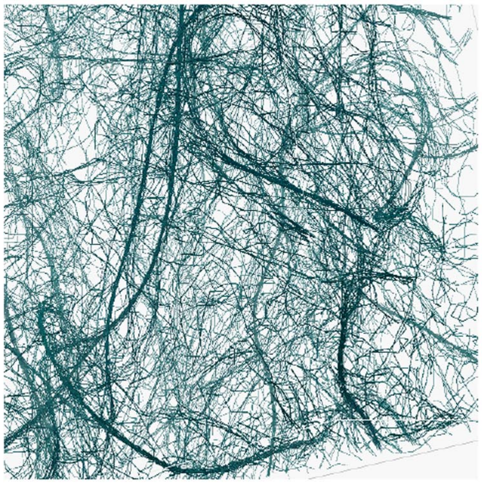

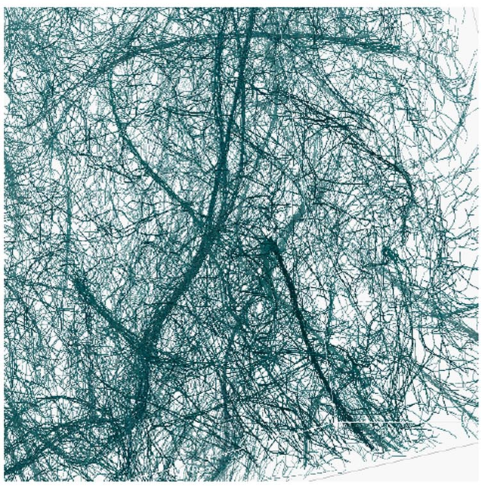

FIG. 3 (color online). Amalgamation of three bundles of superfluid line vortices into a new vortex tube of intensified circulation. In the top figure (left side, $t = 1.3425$ s), two strongly interacting superfluid bundles of aligned vorticity are seen rotating around each other. In the process, they are joined by a third bundle and merge together (bottom, $t = 1.4429$ s) forming a vortex braid. Since the amalgamation process is not complete, the newly formed tube trifurcates at some point along its contour.

friction action and the normal-fluid-like energy spectrum shape is restored.

Computational complexity does not allow us to continue the calculation for much longer times. Nevertheless, the available results suggest that E_s might slowly approach saturation. Indeed, due to the decorrelation between mutual friction action and superfluid vortex dynamics, it is conceivable that (given adequate time) the net energy flow between the two systems could become statistically zero. The associated saturation of the kinematic dynamo would only require that $\langle|Q|\rangle = \langle|F|\rangle = \langle|D|\rangle$ and not necessarily also that $E_s = E_n$. This is a genuinely nonlinear effect, since in magnetohydrodynamics, the linearity of the equation governing the amplified magnetic field does not allow a kinematic MHD dynamo to saturate.

Figure 3 shows the merging of a vortex bundle triad into a new braided vortex of intensified circulation that we alluded before. In connection with the preceding spectrum analysis, it is important to note that the bundle merging process terminates concurrently with the start of the superfluid energy reduction discussed previously (Fig. 2). Since, due to the weakness of mutual friction, such processes are mainly driven by Biot-Savart interactions, they could also be essential for coherent structure formation in normal fluid turbulence.

Calculations were also attempted for $\mathrm{Re}_\gamma = 10^4$ and $T = 1.3$ K, as well as $\mathrm{Re}_\gamma = 40$ and $T = 2.171$ K with similar conclusions.

This work was supported by EPSRC. I thank Anthony Youd and especially Antony Mee for assistance with the graphics.

[1] *Quantized Vortex Dynamics and Superfluid Turbulence*, C. F. Barenghi, R. J. Donnelly, and W. F. Vinen (Springer Verlag, Berlin, 2001).

[2] W. F. Vinen and J. J. Niemela, J. Low Temp. Phys. **128**, 167 (2002).

[3] Z.-S. She and S. A. Orszag, Nature (London) **344**, 226 (1990).

[4] A. Vincent and M. Meneguzzi, J. Fluid Mech. **225**, 1 (1991).

[5] M. Farge, G. Pellegrino, and K. Schneider, Phys. Rev. Lett. **87**, 054501 (2001).

[6] D. Kivotides and A. Leonard, Phys. Rev. Lett. **90**, 234503 (2003).

[7] D. Kivotides and A. Leonard, Europhys. Lett. **65**, 344 (2004).

[8] D. Kivotides and A. Leonard, Europhys. Lett. **66**, 69 (2004).

[9] D. Kivotides, Phys. Lett. A **318**, 574 (2003).

[10] D. Kivotides, JETP Lett. **80**, 152 (2004).

[11] O. C. Idowu, D. Kivotides, C. F. Barenghi, and D. C. Samuels, J. Low Temp. Phys. **120**, 269 (2000).

[12] D. Kivotides and A. Leonard, Europhys. Lett. **63**, 354 (2003).

[13] A. Tsinober, *An Informal Introduction to Turbulence* (Kluwer Academic, Dordrecht, 2001).

[14] *New Trends in Turbulence*, M. Lesieur, A. Yaglom, and F. David (Springer-Verlag, Berlin, 2001).